Author(s): Kotila, Jenni-Mari; Lenzi, Silvia M.

Title: Collective features of Cr and Fe isotopes

Year: 2014

Version:

Please cite the original version:

Kotila, J.-M., & Lenzi, S. M. (2014). Collective features of Cr and Fe isotopes. Physical Review C - Nuclear Physics, 89(6), Article 064304. https://doi.org/10.1103/PhysRevC.89.064304

Collective features of Cr and Fe isotopes

J. Kotila[1,2,*] and S. M. Lenzi[3,†]

[1]*Center for Theoretical Physics, Sloane Physics Laboratory, Yale University, New Haven, Connecticut 06520-8120, USA*

[2]*Department of Physics, University of Jyväskylä, B.O. Box 35, FIN-40014 Jyväskylä, Finland*

[3]*Dipartimento di Fisica e Astronomia, Universitá degli Studi di Padova, and INFN, Sezione di Padova, via F. Marzolo 8, 35131 Padova, Italy*

(Received 27 February 2014; revised manuscript received 5 May 2014; published 9 June 2014)

The question of the sudden increase of collectivity in neutron-rich nuclei when approaching $N = 40$ has recently interested both experimentalists and theorists. In this paper we study the development of collectivity along the chromium and iron isotopic chains. The calculations are performed within two different perspectives, namely, the proton-neutron interacting boson model (IBM-2) and interacting shell model (ISM) and compared with the available experimental data. The onset of collectivity is studied through nuclear quantities and observables that suggest differences in the nuclear structure of Cr and Fe isotopical chains. Furthermore, a prediction for the shape transition from a spherical vibrator to γ-soft rotor with nucleus ^{58}Cr standing at the critical point is discussed.

DOI: 10.1103/PhysRevC.89.064304 PACS number(s): 21.10.Re, 21.60.Ev, 21.60.Fw, 21.60.Cs

I. INTRODUCTION

The continuous experimental developments nowadays allow the study of exotic nuclei with extreme ratios of N/Z. Neutron-rich nuclei are of current interest because of clear indications that the traditional magic numbers of the shell structure near stability are not always preserved far from stability, in particular in light and medium-light nuclei (e.g., Refs. [1–5]). Unstable nuclei in this region exhibit many interesting phenomena such as the appearance of new magic numbers and the development of new regions of deformation for proton or neutron numbers that are magic near stability. In particular, for heavy Cr and Fe nuclei, there is a sudden increase in the collectivity approaching $N = 40$, as observed from the lowering of the energies of the 2_1^+ states and the sudden increase of the quadrupole transition probabilities to the ground state in the neutron-rich even-even isotopes [6–14].

The observed changes help to understand specific terms of the effective nucleon-nucleon interaction and to improve our knowledge of the nuclear structure evolution towards the drip lines. In particular, the relevant role of the monopole part of the tensor force of the proton-neutron interaction in the shell evolution has been discussed in Refs. [2,5,15]. This term causes the changes in the effective single-particle energies that may favor the excitations across the shells. The deformation, on the other hand, is due to the correlations induced by the multipole part of the effective interaction. Recent experimental and theoretical studies have suggested that neutron-rich chromium and iron isotopes around $N = 40$ would lie in a new island of inversion [12–14,16] as was previously found near ^{31}Na at $N \simeq 20$ [17–20]. The increase in collectivity at $N = 40$ is caused by the excitation of neutrons from the pf shell to both the $g_{9/2}$ and $d_{5/2}$ orbitals of the upper main shell [4,16]. These two orbitals form a quasi-SU3 space able to generate quadrupole collectivity, as discussed in Ref. [21]. In addition, neutron particle-hole excitations induce the reduction of the proton $Z = 28$ shell gap due to the proton-neutron interaction, favoring further the development of well-deformed states.

The interacting shell model (ISM) is the most powerful tool for providing a microscopic description of the data and the new experimental information on nuclei far from stability constitutes a challenging test for the applicability of the model. For any such calculation, the two main ingredients are the effective interaction and the model space for valence particles. The particular issue of collectivity at $N = 40$ has previously been a subject of many shell model calculations using different valence spaces and interactions [4,6,16,22,23]. In this work we report the results obtained using a significantly large model space and the recently developed LNPS interaction [16].

A different approach to describe collective properties in nuclei is the interacting-boson model (IBM) [24], which has been extensively used to study medium-mass and heavy nuclei. In particular, the neutron-proton (IBM-2) version of the model has been applied successfully to the light isotopes of Se, Kr, and Sr [25–30]. In Ref. [31] even lighter nuclei, namely ^{54,56}Cr and ^{56,58}Fe, were studied using a method where IBM-2 parameters were derived from a realistic ISM Hamiltonian and transition operators.

The present work was motivated by the question of how well the phenomenological IBM-2 can reproduce the new experimental data and the sudden increase of collectivity in the middle of the proton pf shell, in Cr and Fe nuclei and to compare it with microscopic ISM calculations. Furthermore, our aim is to gain information about the predictive power of these two models in this challenging region by using as simple foundation as possible. For ISM calculation this means using the same effective interaction for all nuclei of current interest and for the IBM-2 calculation, taking only three parameters to be fitted. In this respect, we perform IBM-2 and ISM calculations to assess their ability to describe the onset of deformation in a series of even-even neutron-rich chromium and iron isotopes. We first discuss the theoretical background for both approaches, and compare the level energies, $E2$ transition probabilities and quadrupole moments in the isotopes

*jenni.kotila@yale.edu

†lenzi@pd.infn.it

$^{54–64}$Cr and $^{56–66}$Fe. Additional motivation of this paper is to test the qualities of both approaches in describing the nucleus ^{58}Cr, which has been pointed out as a good candidate for the critical point of the shape phase transition E(5) [32], by comparing the measurable observables resulting from the two calculations with the available experimental data.

The paper is organized as follows. In Sec. II we give a theoretical description, followed by the obtained results and the discussion in Sec. III. Conclusions and outlook for possible future studies are given in Sec. IV.

II. THEORETICAL DESCRIPTION

A. Shell model valence space and effective interaction

A very important improvement for the description of the rapid evolution along the isotopic and isotonic chains when approaching $N = 40$ has been recently achieved by the development of the LNPS interaction [16]. This allows not only to describe the collective structure in nuclei below ^{68}Ni but also heavier nuclei such as the recently studied Cu and Zn isotopes [33–36]. Such a description implies to consider a wide shell model space that involves more than one main shell.

While Cr isotopes up to $N = 34$ can be well described within the pf shell, neutron-rich Fe isotopes up to $N = 36$ need the inclusion of the $g_{9/2}$ neutron orbital in the model space (^{48}Ca core) [23]. This latter model space is also good enough to account for the spectroscopy of moderately neutron-rich Mn [37] isotopes. However, when approaching $N = 40$ these fpg calculations fail to describe the structure of neutron-rich nuclei, in particular, $^{60–62}$Cr [6,8,38] and ^{66}Fe [23].

It is the inclusion of the neutron $d_{5/2}$ orbital which favors quadrupole correlations and the development of quadrupole collectivity in this mass region, as suggested already in Ref. [4]. This can be explained in terms of the quasi-SU3 approximate symmetry: The deformation can be generated by the interplay between the quadrupole force and the central field in the subspace consisting on the lowest $\Delta j = 2$ orbitals of a major shell [21].

The LNPS interaction has been obtained by adapting a realistic CD-Bonn potential after many-body perturbation techniques [39] and monopole modifications. The model space includes the fp shell for protons and the $1p_{3/2}, 1p_{1/2}, 0f_{5/2}, 0g_{9/2}$, and $1d_{5/2}$ orbitals for neutrons. In the present calculation we choose this valence space for the heavy isotopes, while for Cr isotopes with neutron numbers $N = 30$–34 and for Fe isotopes with neutron numbers $N = 30$–32, only the full fp shell was chosen for both protons and neutrons. In all cases the effective charges $e_\pi = 1.31e$ and $e_\nu = 0.46e$ [40] have been used.

B. The IBM-2 Hamiltonian

The IBM in its original version is comprised of the monopole ($L = 0^+$) s and the quadrupole ($L = 2^+$) d bosons, which represent the collective pairs of valence nucleons. In the present work, we employ the proton-neutron interacting boson model (IBM-2), which has microscopic foundation rooted in the spherical shell model. Compared to shell model, in IBM-2 the model space is truncated to include only the so-called proton (neutron) s_π (s_ν) bosons and the d_π (d_ν) bosons thus simplifying the calculations considerably. Since the number of valence protons (neutrons) is fixed for a nucleus, the number of proton (neutron) bosons, denoted as N_π (N_ν), equals half the number of valence protons (neutrons). Eigenstates of quadrupole collective states of interest are generated by the diagonalization of the boson Hamiltonian composed of the basic interactions.

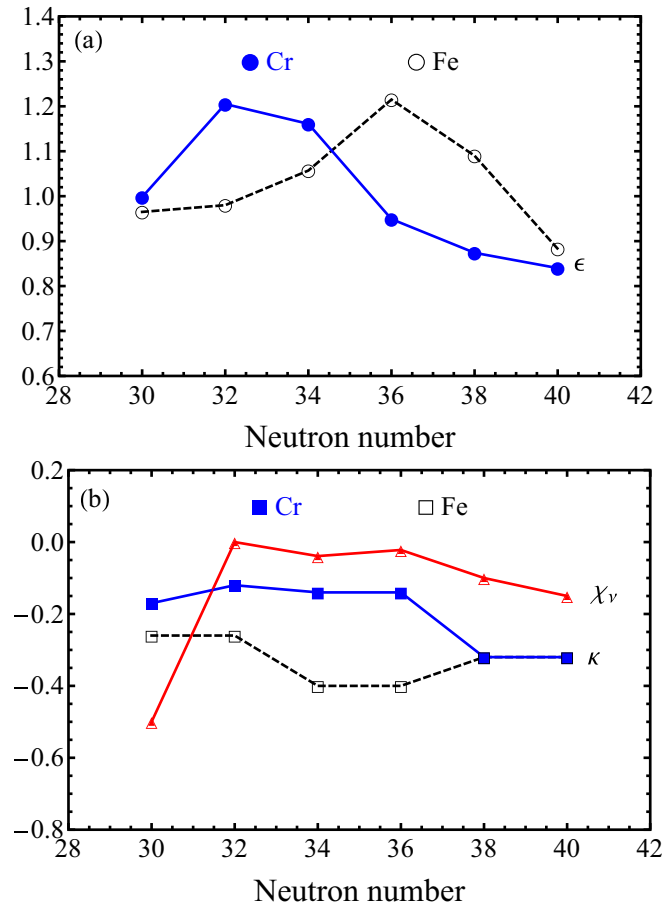

FIG. 1. (Color online) The IBM-2 parameters (a) ϵ(MeV) and (b) κ(MeV) and χ_ν for the considered nuclei.

In the present work, the ^{48}Ca doubly magic nucleus is taken as a boson vacuum for the considered $^{54–64}$Cr and $^{56–66}$Fe nuclei. Thus, the neutron boson number N_ν varies from 1 to 5 for both Cr and Fe, corresponding to the $N = 30$–40 isotopes, respectively. The proton boson number N_π is fixed: $N_\pi = 2$ and 3 for Cr and Fe isotopes, respectively. We first consider the following Hamiltonian, which is often used in the literature and which is general enough for phenomenological studies:

$$\hat{H} = \epsilon(\hat{n}_{d_\pi} + \hat{n}_{d_\nu}) - \kappa \hat{Q}_\pi^{\chi_\pi} \cdot \hat{Q}_\nu^{\chi_\nu} + \lambda \hat{M}_{\pi\nu}, \quad (1)$$

where $\hat{n}_{d_\rho} = d_\rho^\dagger \cdot \tilde{d}_\rho$ and $\hat{Q}_\rho^{\chi_\rho} = s_\rho^\dagger \tilde{d}_\rho + d_\rho^\dagger \tilde{s}_\rho + \chi_\rho [d_\rho^\dagger \tilde{d}_\rho]^{(2)}$ represent the d-boson number operator and the quadrupole operator for proton ($\rho = \pi$) and neutron ($\rho = \nu$), respectively. The parameter χ_ρ, which appears in the quadrupole operator, determines the type of the deformation, i.e., the softness in γ

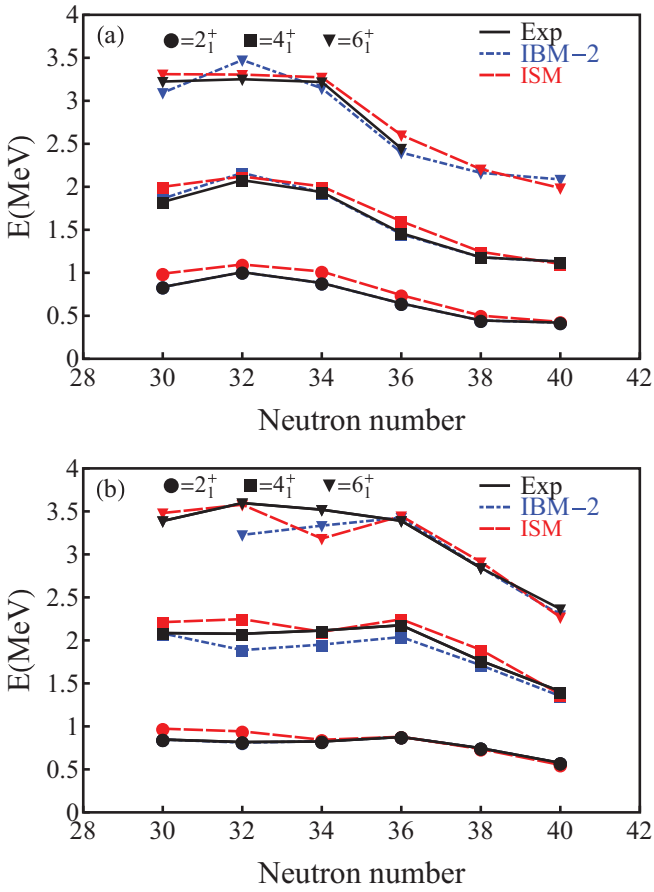

FIG. 2. (Color online) Evolution of the ground state band energies in (a) $^{54-64}$Cr and (b) $^{56-66}$Fe. The IBM-2 2_1^+ energies coincide with the experimental energies.

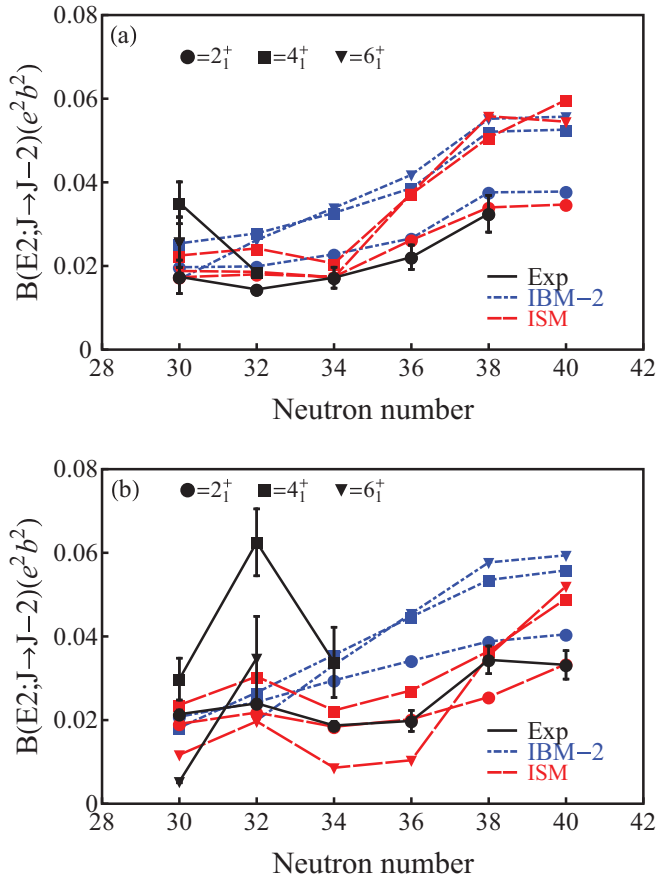

FIG. 3. (Color online) Evolution of the reduced transition probabilities $B(E2; J \rightarrow J-2)$ (e^2b^2) in (a) $^{54-64}$Cr and (b) $^{56-66}$Fe.

degrees of freedom, depending on its sign as well as magnitude. The third term on the right-hand side of Eq. (1) represents the so-called Majorana term, with its strength λ, given as

$$\hat{M}_{\pi\nu} = -2 \sum_{k=1,3} [d_\pi^\dagger d_\nu^\dagger]^{(k)} \cdot [\tilde{d}_\pi \tilde{d}_\nu]^{(k)} + [d_\pi^\dagger s_\nu^\dagger - s_\pi^\dagger d_\nu^\dagger]^{(2)} \cdot [\tilde{d}_\pi \tilde{s}_\nu - \tilde{s}_\pi \tilde{d}_\nu]^{(2)}. \quad (2)$$

The Majorana term is relevant to the proton-neutron mixed symmetry, and has been considered, e.g., in the context of the isovector collective motion of valence nucleons. There are several different notations for the Majorana parameters, we take the one used by Caprio and Iachello [41].

The set of parameters for the IBM-2 Hamiltonian in Eq. (1) is determined for the individual nuclei through the usual fitting procedure starting at the basic experimental data available. In this paper we are not interested on fitting all the data precisely by employing additional parameters but rather finding a reasonable agreement taking as simple parameters as possible and thus profiting to predictive power. That is, the Hamiltonian parameters other than ϵ, κ, and χ_ν are fixed: For Cr (Fe) isotopes, $\chi_\pi = -0.6$ (-0.4), while $\lambda = 0.04$ MeV for both isotopic chains. The parameter χ_ν is taken to be only dependent on N. However, one should note that at odds with the recently studied Gd and Dy case [42], a separate set of ϵ and κ parameters are needed for Cr and Fe isotopes, suggesting that they have rather different structure, although they are neighboring isotopic chains. The evolution of the relevant parameters is shown in Fig. 1. One should note that the scale of panel a) is chosen to emphasize the difference between these two isotopic chains and starts from 0.6 MeV instead of the usual 0.0 MeV. Judging by the parameter ϵ, which essentially determines the excitation energy of the 2_1^+ state, the increase of collectivity takes place at $N \sim 36$ for Cr isotopes and at $N \sim 38$ for Fe isotopes, in agreement with shell model predictions [16]. The ϵ values are notably diverse for the different isotopic chains. Similar behavior is also seen for the values of the parameter κ, which is related to the ratio $R_{4/1} = 4_1^+/2_1^+$ that will be discussed later. Considerably larger absolute values of κ are needed for Fe than for Cr at $N = 34,36$. For boson effective charges we have used values $e_\pi = 0.096$ and $e_\nu = 0.032$ for Cr isotopes, and $e_\pi = 0.141$ and $e_\nu = 0.047$ for Fe isotopes (in eb units).

III. RESULTS

Recent data on the neutron-rich Cr and Fe isotopes show a compression of the 2_1^+ and 4_1^+ energies relative to the lighter isotopes, suggesting the onset of collectivity associated with deformation. IBM-2, as well as, ISM calculations reproduce

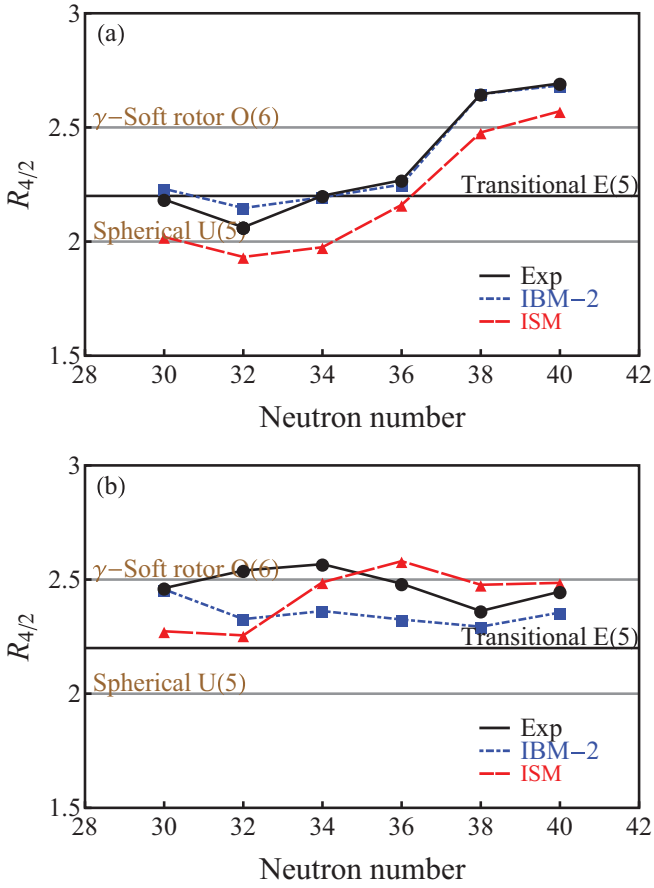

FIG. 4. (Color online) Evolution of the ratio $R_{4/2} = E_x(4_1^+)/E_x(2_1^+)$ in (a) $^{54-64}$Cr and (b) $^{56-66}$Fe.

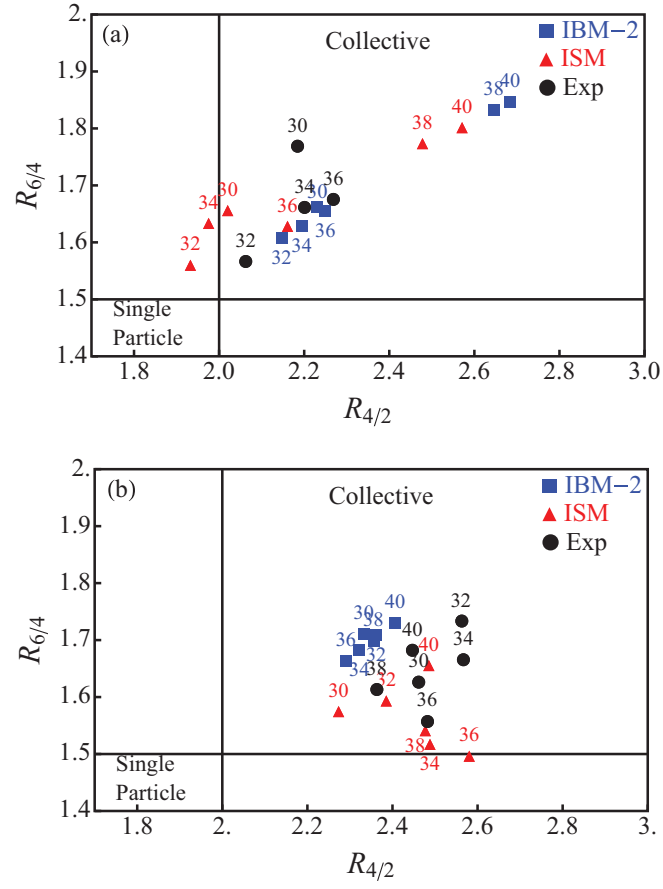

FIG. 5. (Color online) Evolution of the ratio $R_{6/4} = E_x(6_1^+)/E_x(4_1^+)$ as a function of ratio $R_{4/2} = E_x(4_1^+)/E_x(2_1^+)$ in (a) $^{54-64}$Cr and (b) $^{56-66}$Fe.

the measured yrast level structure as is shown in Fig. 2. In general, an equally good agreement with experimental data is found by both models.

Another indicator of increased collectivity are the $B(E2)$ reduced transition strengths, shown in Fig. 3 for the ground state band transitions. Both theoretical methods are in good agreement with the available experimental data [43], which is, however, very limited. An exception is the $B(E2; 4_1^+ \to 2_1^+)$ value in ^{58}Fe which experimental value is exceptionally large. Chromium isotopes show a smooth behavior with increasing collectivity as N increases. For the iron isotopes IBM-2 predicts also a rather smooth behavior conflicting with data [13,14], which shows a rapid increase at $N = 38$. On the other hand, ISM calculations give an excellent agreement for $B(E2; 2_1^+ \to 0_1^+)$ transition probabilities, except for $N = 38$. For the other transitions there is not enough experimental data available for conclusions. A clear increase of collectivity is seen for Cr as increasing $B(E2)$ values when approaching the middle of the shell, as expected. For Fe isotopes the situation is more complicated, and no consistent behavior is observed.

The ratio $R_{4/2} = E_x(4_1^+)/E_x(2_1^+)$, shown in Fig. 4, between the 2_1^+ and 4_1^+ energies provides a convenient classification of structural properties in terms of noncollective (<2.0), spherical-vibrational (∼2.0), transitional (∼2.5), or rigid-rotor (∼3.33) regimes. Experimental $R_{4/2}$ ratio shows transitional character between $N = 30$ and 36 in the Cr isotopic chain. In contrast, it remains rather constant in the corresponding Fe chain. The difference in the $R_{4/2}$ ratio points to a different intrinsic structure for the two isotopic chains. This result was also recently discussed in Ref. [7]. In the current study both models reproduce the rapid rise for Cr isotopes in $R_{4/2}$. IBM-2 also pins the $N = 34$ to the E(5) critical point limit [32] similar to the data, whereas ISM suggest that the $N = 36$ would be closer to the E(5) limit. In Fe isotopes neither of the models are able to follow the experimental trend of the $R_{4/2}$ for $N < 36$. For $N = 30$, IBM-2 agrees with the data but systematically underestimates the $R_{4/2}$ for increasing N, while ISM underestimates the value of the ratio for lighter isotopes and overestimates it for the heavier ones.

Another informative ratio $R_{6/4} = E_x(6_1^+)/E_x(4_1^+)$ as a function of $R_{4/2}$ is shown in Fig. 5. Collective structures should resemble a line with a clear slope, as is the case for Cr. Experimental data, as well as the IBM-2 calculation categorize all the discussed chromium isotopes to the collective segment with the collectivity increasing with N. ISM predicts similar behavior with the exception of $N = 34$ nucleus which is very near to spherical nuclei. The highest values are obtained for $N = 40$ in both models. For $N = 38,40$ there is no experimental data about $E_x(6_1^+)$. For iron isotopes the situation

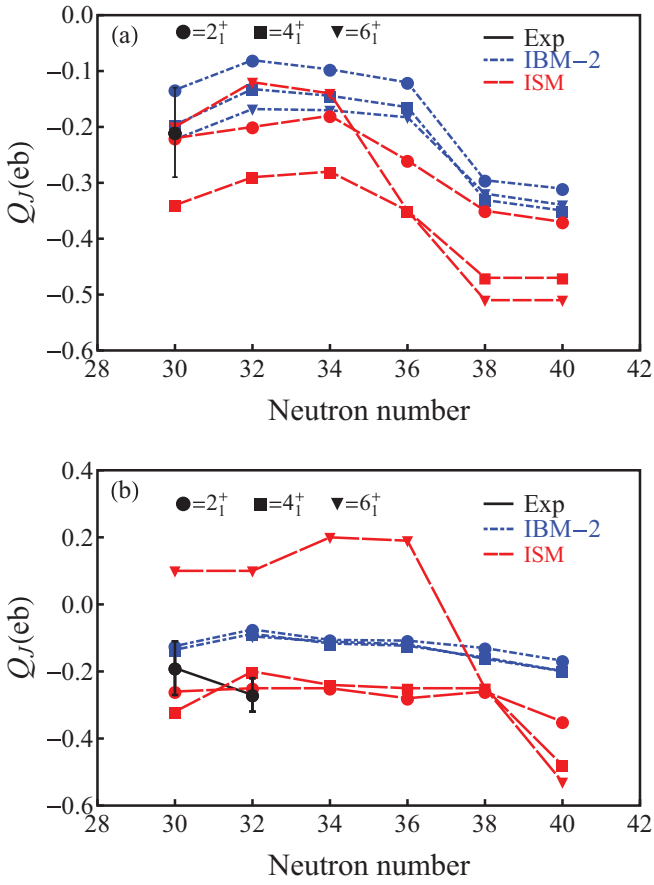

FIG. 6. (Color online) Evolution of the quadrupole moments $Q_{J_1^+}$ in (a) $^{54-64}$Cr and (b) $^{56-66}$Fe.

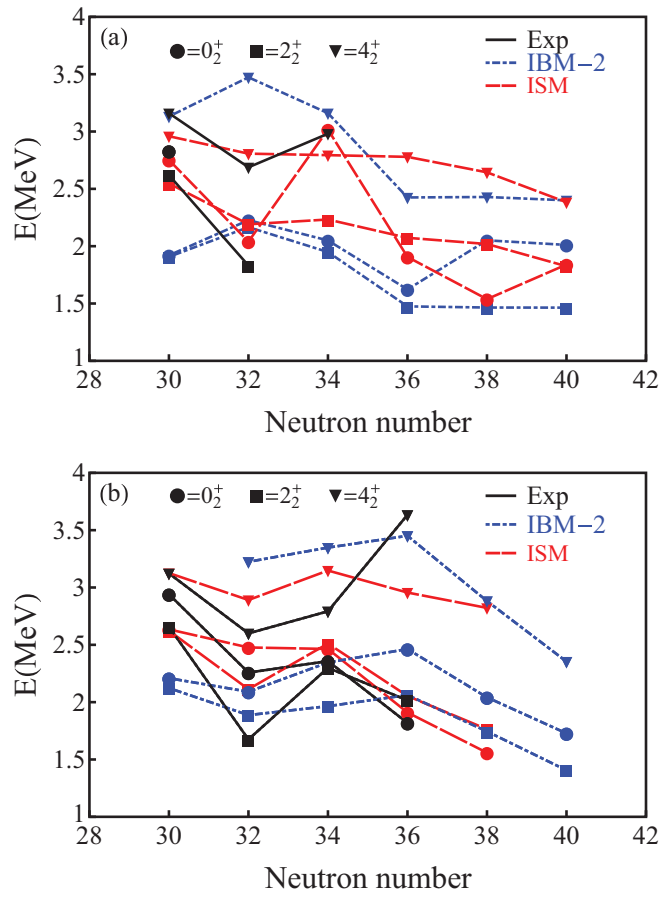

FIG. 7. (Color online) Evolution of the higher lying 0_2^+, 2_2^+, and 4_2^+ state energies in (a) $^{54-64}$Cr and (b) $^{56-66}$Fe.

is again notably different and more gradual and clustered values of $R_{6/4}$ are found. Surprisingly highest value is found at $N = 32$ for experiments. However, it is very near the $N = 40$ value, which also is the highest for both theoretical models.

We then study the quadrupole moments shown in Fig. 6. A good measure of the collective structure are the quadrupole moments, especially for the 2_1^+ excited state, denoted as $Q_{2_1^+}$. The development of the nuclear deformation can be seen from the neutron closed shell at $N = 28$ towards the open-shell nuclei. Experimental data is only available for the $N = 30$ and $N \leq 32$ nuclei for Cr and Fe, respectively, where both theoretical predictions are in acceptable agreement. For heavier chromium isotopes ISM predicts much larger magnitudes for quadrupole moments than IBM-2. The behavior of both predictions is rather smooth for both isotopes. Notable is the sudden increase of the magnitude of $Q_{6_1^+}$ seen in the ISM prediction in ^{62}Cr and ^{64}Fe where the collective nature seems to settle.

For consistency, the behavior of the higher lying 0_2^+, 2_2^+, and 4_2^+ states is presented in Fig. 7, and that of 3_1^+ and 5_1^+ in Fig. 8. Since in our current study we are interested in the predictive power of the used models, it is necessary that also these collective states can be described at least fairly. Experimental data shows a rapid drop in the 0_2^+, 2_2^+, and 4_2^+ energies in both isotones when moving from $N = 30$ to $N = 32$. This behavior is also seen from ISM calculation and IBM-2 calculation for Fe, whereas IBM-2 suggests a slight rise for Cr in these energies. In the case of Cr, for $N > 32$ there is no experimental data available but the predictions of the two models discussed here are rather contradicting for the 0_2^+ state. However, both models predict the lowering of the 2_2^+ and 4_2^+ level energies, with an abrupt fall at $N = 36$ for IBM-2. In the case of Fe, the data shows rather rapid changes, the trend still being the same with both calculations.

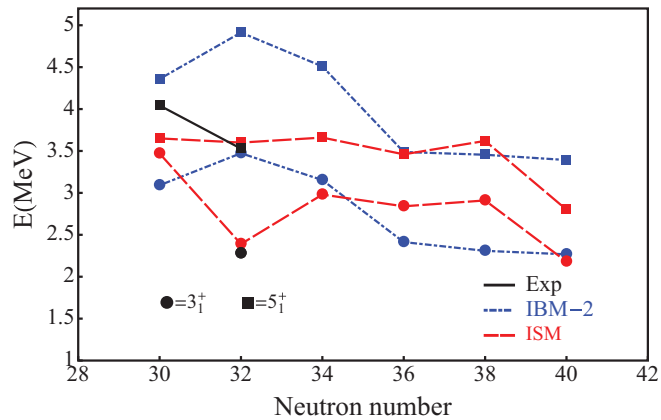

FIG. 8. (Color online) Evolution of 3_1^+ and 5_1^+ state energies in $^{54-64}$Cr.

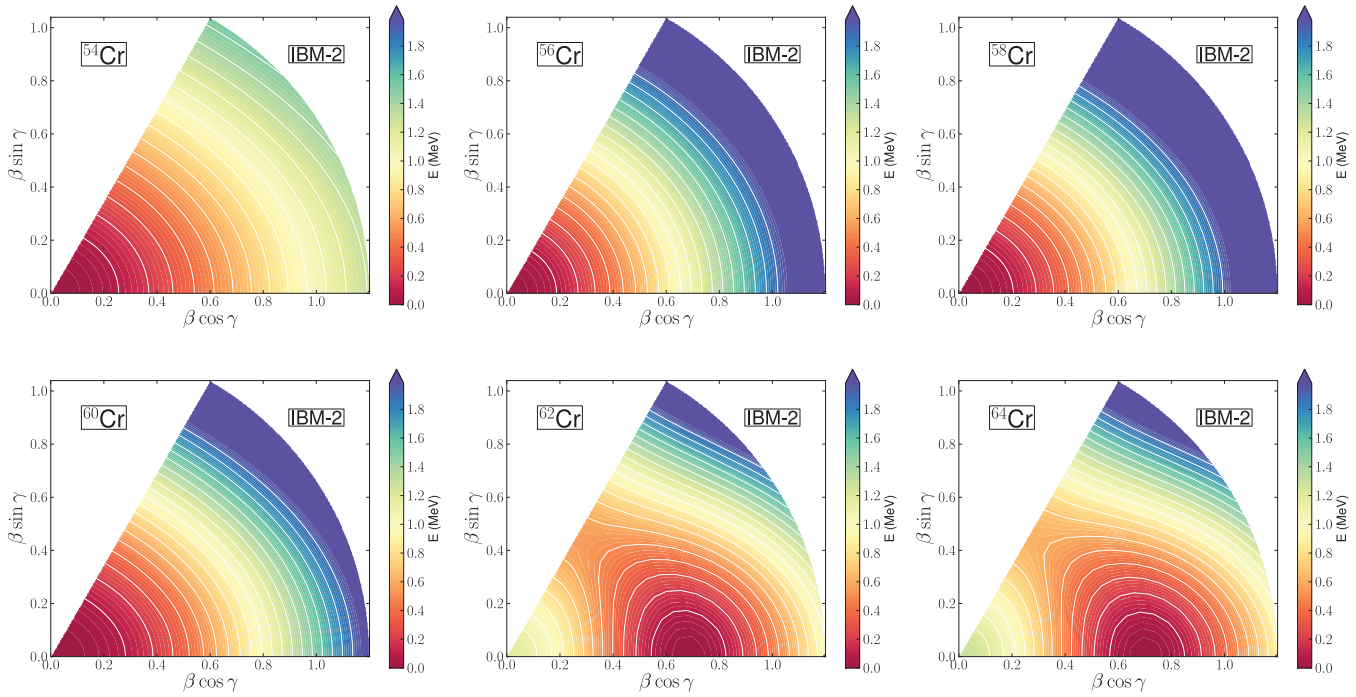

FIG. 9. (Color online) Energy surfaces of the $^{54-64}$Cr nuclei obtained from the IBM-2 Hamiltonian.

The behavior of the 3_1^+ and 5_1^+ states gives a hint on the evolution of the shape along an isotopic chain. In Fig. 8 we plot the 3_1^+ and 5_1^+ states for Cr isotopes. Due to the limited experimental data, the Majorana parameter, that also affects the IBM-2 3_1^+ state energies is not fitted and a constant value of $\lambda = 0.04$ is used for all the studied isotopes as already mentioned earlier. In the case of IBM-2, the energies show a smooth behavior with the lowering starting form $N = 32$, comparable to the behavior of the 2_2^+ and 4_2^+. For IBM-2 the 3_1^+ state lies always lower than, but close in energy to the 4_2^+ state indicating a signature of γ-softness. As was already shown for 0_2^+, 2_2^+, and 4_2^+ states, ISM gives rather different results, still showing the lowering of the 3_1^+ and 5_1^+ energies at $N = 40$.

We finally discuss the phenomenon of shape phase transition in Cr isotopes. Shape phase transition can be studied easily in IBM-2 by constructing potential energy surfaces (e.g., [42]). The energy surfaces for $^{54-64}$Cr and $^{56-66}$Fe nuclei, respectively, are shown in Figs. 9 and 10. In case of Cr isotopes, the change in the absolute minimum of the energy surface points to an evolution from spherical vibrator, $U(5)$, towards a deformed, γ-soft rotor, with ^{58}Cr at the critical point. This is consistent with the shell model calculations which show the second 4^+ state below the 6^+ up to ^{58}Cr and increasingly above it for higher isotopes. A similar behavior is predicted for the 3^+ states. In the case of Fe isotopes the situation is more involved and no conclusion about shape phase transition can be made on this basis.

As discussed above, the experimental data point at an evolution from a spherical vibrator to γ-soft rotor with nucleus ^{58}Cr standing at the critical point limit. This nucleus has also been studied extensively with ISM using different interactions in Ref. [38]. We report in Fig. 11 the experimental spectra of ^{58}Cr in comparison with the predictions of the IBM-2, ISM and the E(5) symmetry. As it can be deduced from Fig. 11, the excitation energies are in very good agreement with the theoretical results, and in particular with the $E(5)$ dynamical symmetry. Differences arise in the $B(E2)$ values. Precise measurements of lifetimes and/or transition probabilities are mandatory to prove the transitional character of ^{58}Cr. Both in connection with the E(5) symmetry in ^{58}Cr and in general with the nature of the wave functions of the states in $^{54-64}$Cr and $^{56-66}$Fe it is of interest to comment on the differences and similarities between IBM-2 and ISM in this region. The ISM provides description of both collective and non-collective states, where IBM-2 provides description of only collective states. The yrast band $0_1^+, 2_1^+, 4_1^+, 6_1^+$ appear to be, in most of the nuclei studies in this paper, collective, as shown by the energies in Fig. 2 and the $B(E2)$ values in Fig. 3, and therefore IBM-2 and ISM give rise to almost identical results. On the other side, while the wave functions of the non-yrast states $0_2^+, 2_2^+, 4_2^+$ are still collective in IBM-2, in the ISM they are either non-collective or a mixture of collective and noncollective, as clearly seen in the right hand side of Fig. 11. For nonyrast states IBM-2 and ISM thus differ considerably. The same comment applies for the nonyrast states 3_1^+ and 5_1^+. Only additional experiments can tell the extent to which collectivity is fully present in this region, either in the form of spherical vibrators, U(5) symmetry, transitional, E(5) symmetry, γ-unstable, O(6) symmetry, or eventually, deformed rotor, SU(3) symmetry. The latter, however is clearly excluded by the existing data, and by both the IBM-2 and ISM calculations in this region.

IV. CONCLUSIONS

The development of collectivity and deformation in the neutron-rich nuclei around $N = 40$ for $Z < 28$, is a subject

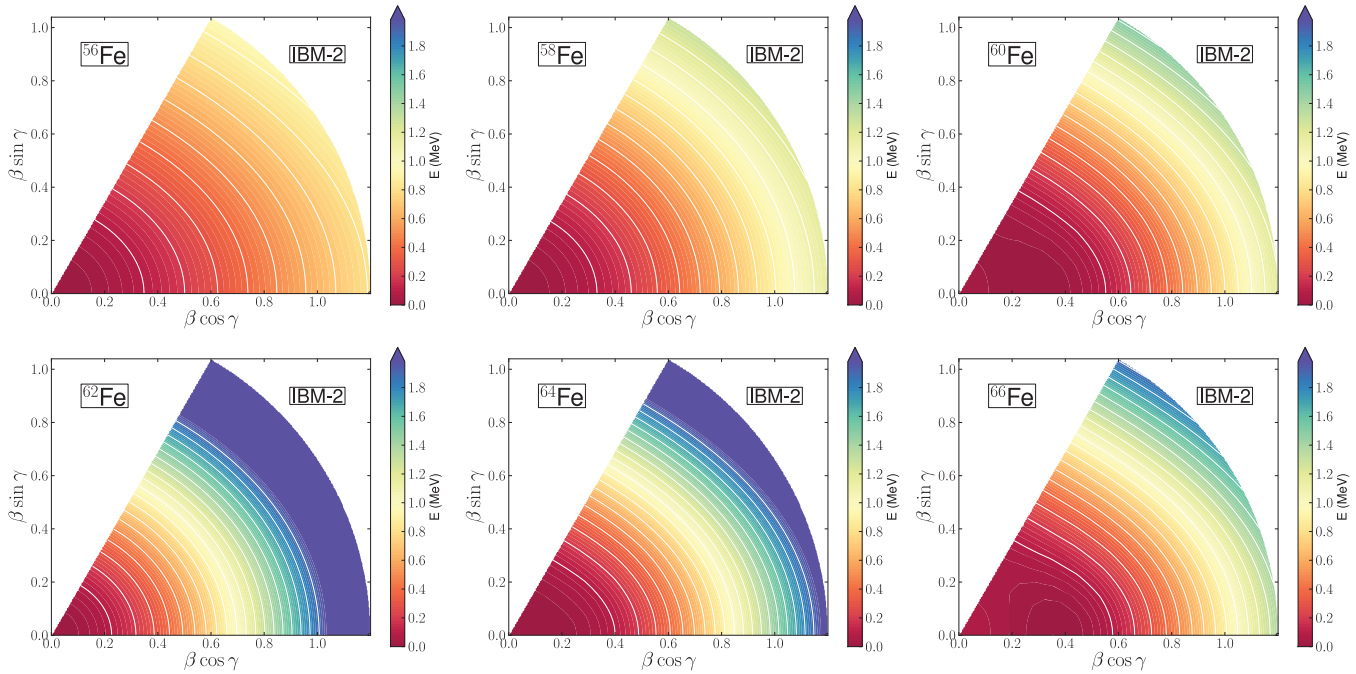

FIG. 10. (Color online) Energy surfaces of the $^{56-66}$Fe nuclei obtained from the IBM-2 Hamiltonian.

of current interest from both the experimental and theoretical points of view. Data are being obtained by means of different experimental techniques providing an excellent testing ground for theoretical models and their ability to describe changes of structure and shapes along isotopic chains, and further, to predict new ones.

The development of collectivity is found to be well reproduced by the two different methods, namely, the phenomenological IBM-2 and the microscopic ISM. Both calculations are performed using simple inputs in order to justify the extension of these calculations to a region where experimental data available is very sparse. The ISM calculation was performed in a model space that included the pf shell for protons and the pf shell or $f_{5/2}$, $p_{3/2}$, $p_{1/2}$, $g_{9/2}$, and $d_{5/2}$ for neutrons, depending on the neutron number. The new effective interaction, LNPS, is able to reproduce the rapid changes of structure in this mass region, together with the phenomena of shape phase transition in Cr nuclei. The IBM-2 calculation was performed using rather simple Hamiltonian where just few parameters were allowed to change. However, this simple procedure is found to give fair agreement with experimental features of this challenging region. The two methods describe equally well the excitation energy of the yrast states in chromium isotopes, as well as the transition probabilities, and the ratios of the excitation energies $R_{4/2}$ and $R_{6/4}$. For the quadrupole moments they agree in the trend of these values but not in the magnitude. Regarding the iron isotopes, they describe well the yrast states but the agreement between the two models gets worse for the other quantities.

The special case of ^{58}Cr shows the characteristic excitation-energy sequence of a critical point of the E(5) shape-phase transition from spherical to γ-unstable rotational regime. The development of deformation in the heavy Cr isotopes is sustained by the predictions of the quadrupole moments and the ratios of the excitation energies of the yrast 2^+,4^+,6^+ states, $R_{4/2}$ and $R_{6/4}$. On the other hand no clear shape evolution is

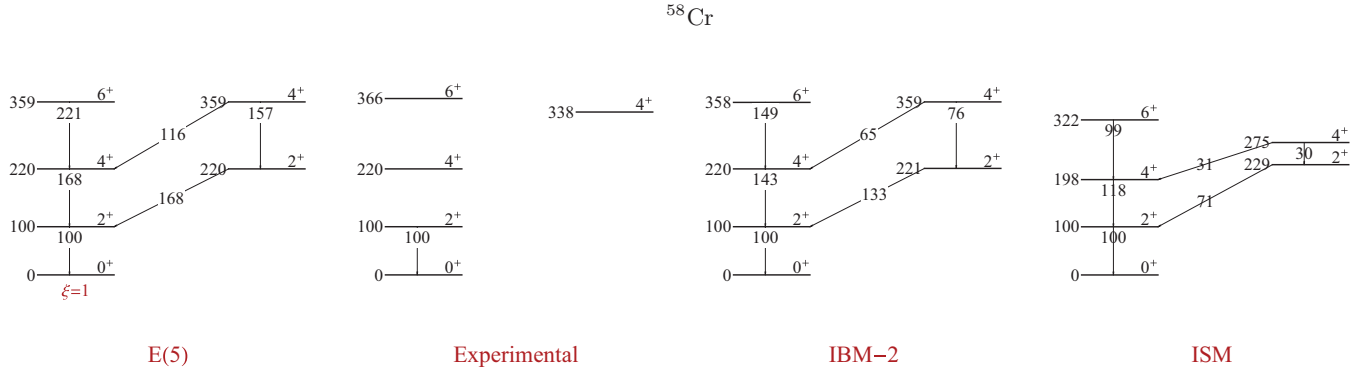

FIG. 11. (Color online) Spectrum of E(5) symmetry compared with experimental and theoretical spectra for ^{58}Cr. Energies are in units of the first excited state, $E_x(2_1^+) = 100$, and $B(E2)$ values are in units of $B(E2; 2_1^+ \rightarrow 0_1^+) = 100$.

observed in Fe isotopes. The increase of deformation suggested by the decrease of the 2_1^+ energy and the increase of the $B(E2)$ values when approaching $N = 40$, is not consistent with the behavior of the quadrupole moments and the energy ratios, indicating a more complex structure than for Cr isotopes. This is consistent with the collectivity dictated by $N_\pi N_\nu$ scheme [44], since the proton number for chromium is exactly in the middle of the 20–28 shell, iron being already near the closed shell. A similar situation should be observed in titanium isotopes, as was recently pointed out in an experimental study [45]. The continuous experimental developments will allow in the future to compare data with IBM-2 and ISM predictions for Ti, Cr, and Fe, when neutron numbers are allowed to span the entire 28–50 shell.

ACKNOWLEDGMENTS

The authors thank Professor F. Iachello for valuable discussions and Dr. K. Nomura for providing the program to plot potential energy surfaces. This work was performed in part under the USDOE Grant No. DE-FG02-91ER-40608 and the Academy of Finland Grant No. 266437.

[1] J. Dobaczewski, I. Hamamoto, W. Nazarewicz, and J. A. Sheikh, Phys. Rev. Lett. **72**, 981 (1994).
[2] T. Otsuka, R. Fujimoto, Y. Utsuno, B. A. Brown, M. Honma, and T. Mizusaki, Phys. Rev. Lett. **87**, 082502 (2001).
[3] B. A. Brown, Prog. Part. Nucl. Phys. **47**, 517 (2001), and references therein.
[4] E. Caurier, F. Nowacki, and A. Poves, Eur. Phys. J. A **15**, 145 (2002).
[5] T. Otsuka, T. Suzuki, R. Fujimoto, H. Grawe, and Y. Akaishi, Phys. Rev. Lett. **95**, 232502 (2005).
[6] O. Sorlin *et al.*, Eur. Phys. J. A **16**, 55 (2003).
[7] A. Gade *et al.*, Phys. Rev. C **81**, 051304(R) (2010).
[8] N. Aoi *et al.*, Phys. Rev. Lett. **102**, 012502 (2009).
[9] M. Hannawald *et al.*, Phys. Rev. Lett. **82**, 1391 (1999).
[10] P. Adrich *et al.*, Phys. Rev. C **77**, 054306 (2008).
[11] H. L. Crawford *et al.*, Phys. Rev. Lett. **110**, 242701 (2013).
[12] T. Baugher *et al.*, Phys. Rev. C **86**, 011305(R) (2012).
[13] J. Ljungvall *et al.*, Phys. Rev. C **81**, 061301(R) (2010).
[14] W. Rother *et al.*, Phys. Rev. Lett. **106**, 022502 (2011).
[15] N. A. Smirnova, K. Heyde, B. Bally, F. Nowacki, and K. Sieja, Phys. Rev. C **86**, 034314 (2012).
[16] S. M. Lenzi, F. Nowacki, A. Poves, and K. Sieja, Phys. Rev. C **82**, 054301 (2010).
[17] C. Thibault, R. Klapisch, C. Rigaud, A. M. Poskanzer, R. Prieels, L. Lessard, and W. Reisdorf, Phys. Rev. C **12**, 644 (1975).
[18] X. Campi, H. Flocard, A. K. Kerman, and S. Koonin, Nucl. Phys. A **251**, 193 (1975).
[19] E. K. Warburton, J. A. Becker, and B. A. Brown, Phys. Rev. C **41**, 1147 (1990).
[20] Y. Utsuno, T. Otsuka, T. Glasmacher, T. Mizusaki, and M. Honma, Phys. Rev. C **70**, 044307 (2004).
[21] A. P. Zuker, J. Retamosa, A. Poves, and E. Caurier, Phys. Rev. C **52**, R1741 (1995).
[22] K. Kaneko, Y. Sun, M. Hasegawa, and T. Mizusaki, Phys. Rev. C **78**, 064312 (2008).
[23] S. Lunardi *et al.*, Phys. Rev. C **76**, 034303 (2007).
[24] F. Iachello and A. Arima, *The Interacting Boson Model* (Cambridge University Press, Cambridge, 1987).
[25] A. F. Barfield and K. P. Lieb, Phys. Rev. C **41**, 1762 (1990).
[26] U. Kaup, C. Möntkemeyer, and P. von Brentano, Z. Phys. A **310**, 129 (1983).
[27] U. Kaup and A. Gelberg, Z. Phys. A **293**, 311 (1979).
[28] K. Heyde, J. Moreau, and M. Waroquier, Phys. Rev. C **29**, 1859 (1984).
[29] T. Matsuzaki and H. Taketani, Nucl. Phys. A **390**, 413 (1982).
[30] H. Higo, S. Matsuki, and T. Yanabu, Nucl. Phys. A **393**, 224 (1983).
[31] H. Nakada and T. Otsuka, Phys. Rev. C **55**, 748 (1997).
[32] F. Iachello, Phys. Rev. Lett. **85**, 3580 (2000).
[33] E. Rapisarda *et al.*, Phys. Rev. C **84**, 064323 (2011).
[34] E. Fiori *et al.*, Phys. Rev. C **85**, 034334 (2012).
[35] C. Louchart *et al.*, Phys. Rev. C **87**, 054302 (2013).
[36] K. Sieja and F. Nowacki, Phys. Rev. C **85**, 051301(R) (2012).
[37] J. J. Valiente-Dobon *et al.*, Phys. Rev. C **78**, 024302 (2008).
[38] N. Mărginean *et al.*, Phys. Lett. B **633**, 696 (2006).
[39] M. Hjorth-Jensen, T. Kuo, and E. Osnes, Phys. Rep. **261**, 125 (1995).
[40] M. Dufour and A. P. Zuker, Phys. Rev. C **54**, 1641 (1996).
[41] M. A. Caprio and F. Iachello, Ann. Phys. (NY) **318**, 454 (2005).
[42] J. Kotila, K. Nomura, L. Guo, N. Shimizu, and T. Otsuka, Phys. Rev. C **85**, 054309 (2012).
[43] For data see http://www.nndc.bnl.gov/ensdf/ and http://www.nndc.bnl.gov/ensdf/ensdf/xundl.jsp
[44] For a review of the $N_\pi N_\nu$ scheme see R. F. Casten and N. V. Zamfir, J. Phys. G: Nucl. Part. Phys. **22**, 1521 (1996).
[45] H. Suzuki *et al.*, Phys. Rev. C **88**, 024326 (2013).